Earthquakes and Structures, *Vol. 14, No. 6 (2018) 525-535*
DOI: https://doi.org/10.12989/eas.2018.14.6.525

Evaluating the accuracy of a new nonlinear reinforced concrete beam-column element comprising joint flexibility

Mehdi Izadpanah[1a] and AliReza Habibi[*2]

[1]*Department of Civil Engineering, Kangavar Branch, Islamic Azad University, Kangavar, Iran*
[2]*Department of Civil Engineering, Shahed University, Tehran, Iran*

(Received November 12, 2017, Revised March 28, 2018, Accepted April 4, 2018)

Abstract. This study presents a new beam-column model comprising material nonlinearity and joint flexibility to predict the nonlinear response of reinforced concrete structures. The nonlinear behavior of connections has an outstanding role on the nonlinear response of reinforced concrete structures. In presented research, the joint flexibility is considered applying a rotational spring at each end of the member. To derive the moment-rotation behavior of beam-column connections, the relative rotations produced by the relative slip of flexural reinforcement in the joint and the flexural cracking of the beam end are taken into consideration. Furthermore, the considered spread plasticity model, unlike the previous models that have been developed based on the linear moment distribution subjected to lateral loads includes both lateral and gravity load effects, simultaneously. To confirm the accuracy of the proposed methodology, a simply-supported test beam and three reinforced concrete frames are considered. Pushover and nonlinear dynamic analysis of three numerical examples are performed. In these examples the nonlinear behavior of connections and the material nonlinearity using the proposed methodology and also linear flexibility model with different number of elements for each member and fiber based distributed plasticity model with different number of integration points are simulated. Comparing the results of the proposed methodology with those of the aforementioned models describes that suggested model that only uses one element for each member can appropriately estimate the nonlinear behavior of reinforced concrete structures.

Keywords: material nonlinearity; joint flexibility; spread plasticity; lateral load; gravity load

1. Introduction

Reinforced Concrete (RC) structural components have various influences and complicated features. Although simulating all of these effects is necessary to achieve an accurate prediction of nonlinear responses in RC structures, its time-consuming and calculus complexity make high computational cost for analysis. Among different features, the nonlinear behavior of connections as well as material nonlinearity including concrete cracking and plasticity of reinforced concrete are some crucial causes incensing observed nonlinear behavior in reinforced concrete frames.

A rigid behavior for beam-column connections is usually considered in the numerical analysis of RC structures. This assumption can cause incorrect outcomes in forecasting the nonlinear responses of these structures. To achieve more realistic estimation for the inelastic behavior of RC structures, simulating the nonlinear behavior of connections is necessary. Slippage of the flexural reinforcement and influence of it on the relative rotation between beam and column or the global behavior of the connections was evaluated by some research such as Paulay and Scarpas (1981), Filippou *et al*. (1983), Alameddine and Ehsani (1991). Kitayama *et al*. (1987), Park and Ruitong (1998), Walker (2001) showed that damage of joints can decrease the frame strength and stiffness. Russo *et al*. (1990), Monti *et al*. (1997) and some other research presented some analytical methods to simulate the bond behavior in finite element approach. Altoontash and Deierlein (2003), Mitra and Lowes (2007) used a finite volume joint element connected to one dimension beam and column elements. Ghobarah and Biddah (1999), Lowes and Altoontash (2003), Birely *et al*. (2012) used two springs to represent the relative rotation developed by the slippage of reinforcement and the shear distortion of the joint. Although simplicity and low computational effort of these models are the advantages of them, their requirement to calibrate the entry parameters is the significant obstacle of widespread usage of them (Alva and El Debs 2013). Sezen and Moehle (2003), Sezen and Setzler (2008), Zhao and Sritharan (2007) evaluated the rotation made by the slippage of the tensioned reinforcement of column anchored in the foundation. Pautre *et al*. (1989), Kwak and Kim (2010), Alva and El Debs (2013) proposed some simple analytical models. The used parameters in these studies are according to usual data for design; therefore, these models are more practical for applying in structural analysis. Masi *et al*. (2013), Shafaei *et al*. (2014) evaluated the seismic behavior of RC beam-column joints. Masi *et al*. (2013) evaluated the effects of the value of the axial load acting on the column and the failure of beam longitudinal rebars on the collapse mode. Shafaei *et al*. (2014) assessed the influence of slip of

∗Corresponding author, Associate Professor
E-mail: ar.habibi@shahed.ac.ir
[a]Ph.D.
E-mail: m.izadpanah@iauksh.ac.ir

http://www.techno-press.com/journals/eas&subpage=7
ISSN: 2092-7614 (Print), 2092-7622 (Online)

the beam longitudinal reinforcement in the joint and shear deformation of joint panel on the rigidity of the joint. They concluded that the lateral load carrying capacity of frames is reduced and fundamental period is increased by modeling joint flexibility. In this study, the proposed analytical model by Alva and El Debs (2013) is used to derive moment-rotation relationship of RC beam-column connections. In fact, compatibility of the results with experimental ones and no requirement for calibration the entry parameters are two main advantages of this model.

To simulate plastification of structures simply and efficiently, some macro-models have been presented to date. These models fall into two categories: lumped plasticity and distributed plasticity. In the former, variation of stiffness and strength is traced in predefined plastic hinges at the ends of the member (Kunnath and Reinhorn 1989, Inel and Ozmen 2006, Birely *et al*. 2012, Zhao *et al*. 2012, Amorim *et al*. 2013, Rahai and Nafari 2013, Babazadeh *et al*. 2016). In spite of simplicity and low computational effort of these models, lumped plasticity models are not compatible with RC members because once a RC member experiences inelastic deformation, cracks tend to spread along the member and stiffness becomes non-uniform. In the latter, plasticity is distributed along the member and stiffness matrix components are acquired based on prescribed flexibility patterns in inelastic zones (Scott and Fenves 2006, Kim and Kurama 2008, Lee and Filippou 2009, Roh *et al*. 2012, Nguyen and Kim 2014, Mazza 2014, Pan *et al*. 2016). Linear and uniform flexibility models are two prevalent models for RC structures that in both models, the flexibility solely varies in inelastic zones while the rest of the member remains elastic (Kunnath and Reinhorn 1989). Izzuddin *et al*. (1994), proposed the effective analysis of reinforced concrete frames. They presented a quartic formulation in which the effects of concrete tensile cracking, the nonlinear compressive response of concrete and the beam-column action were simulated. Comparison of their presented model with the nonlinear analysis program ADAPTIC confirmed the accuracy of their model. Tsonos (2007) studied the cyclic load behavior of reinforced concrete beam-column subassemblages of modern structures. He evaluated four one-half scale specimens subjected to a large number of inelastic cycles. The outcomes showed that current design procedures could result in too much damage to the joint regions and even premature lateral instability for moment-resisting frames. Tsonos (2008) evaluated the influence of a reinforced concrete jacket and a high-strength fiber jacket for cases of post-earthquake and pre-earthquake retrofitting of columns and beam-column joints experimentally and analytically. The results indicated that in the case of post-earthquake retrofitting of columns and b/c joints, the reinforced concrete jacket was more efficient whereas, in the case of pre-earthquake strengthening, a reinforced concrete jacket and a high-strength fibre jacket were similar. Lee and Filippou (2009) presented an effective beam-column element with variable inelastic end zones to increase the accuracy of the previous models that considered the fixed length of the inelastic zones. Tsonos (2010) studied the efficiency of shotcrete and cast-in-place concrete. He examined the efficiency of four-sided and two-sided reinforced shotcrete or cast-in-place concrete jackets experimentally and concluded that all types of concrete jackets have the same ability to strengthen existing old frame structures. Roh *et al*. (2012) proposed a power spread plasticity model. They proved that the high order spread plasticity models produce smaller displacement and higher acceleration in the inelastic analysis of the reinforced concrete structures. Disregarding the gravity load effect and not separating the cracked and yielded lengths are two important shortcomings of the proposed distributed plasticity models that can bring about incorrect results as illustrated by Izadpanah and Habibi (2015).

The main objective of this study is to develop a new RC beam-column element in which the distributed plasticity and joint flexibility are taken into consideration. It is worth emphasizing that in some previous studies (Filippou *et al*. 1992, Mergos and Kappos 2012, Mashaly *et al*. 2011), several beam-column elements have been introduced for accounting the material nonlinearity and joint deformability. Requirement to calibrate the entry parameters to simulate the nonlinear behavior of connections is one of the drawbacks of these elements. Another disadvantage of the previous beam-column elements is related to modeling the material nonlinearity because these proposed beam-column elements usually simulate the plasticity of the element using either concentrated plasticity models or simple spread plasticity models that both of them have some disadvantages as explained before. In this study, the proposed relations of Alva and El Debs (2013) are used to model the flexural joint deformability. Moreover, plasticity is distributed throughout along the member applying the methodology that was proposed by Izadpanah and Habibi (2018). In the aforementioned methodology, both gravity and lateral load effects are considered. Also the cracked and yielded lengths are considered as segregated. To verify the correctness of the proposed RC beam-column element, a simply-supported beam and three reinforced concrete moment resistant frames are considered. First, the load-deflection response of the beam under monotonic loading is obtained using the proposed methodology and the outcomes are compared with those of an experimental test and finite element analysis. Then, the ten-story, two-bay frame is considered and the results of the proposed methodology are compared with IDARC2D (Reinhorn *et al*. 2009) platform as a well-known computer package that has been used in many researches such as Roh *et al*. (2012), Lee and Woo (2002), Habibi and Moharrami (2010), Izadpanah and Habibi (2018), Ismail and Zamahidi (2015), Habibi (2008), Sivaselvan and Reinhorn (2000), Sun *et al*. (2011). Afterwards, the outcomes of the proposed model are contrasted with the results of OpenSees software framework system (Mazzoni *et al*. 2007) as a well-known computer package that has been applied in many researches such as Berry *et al*. 2008, He and Zhong (2012), Scott *et al*. (2008), Rahai and Nafari (2013), Gu *et al*. (2011), Lee and Filippou (2009), Mazza (2014), for two reinforced concrete moment resisting frames. For these examples, to evaluate the effect of joint flexibility on the response of RC frames, analyses are performed twice, once with considering rigid behavior

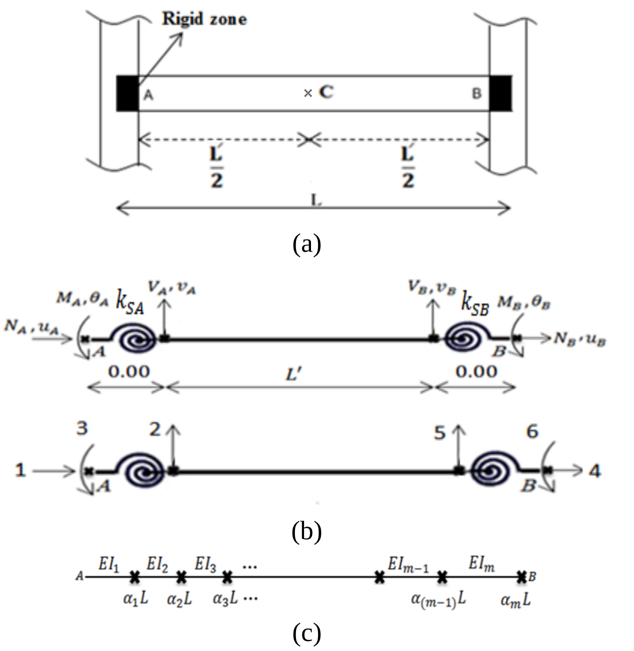

Fig. 1 (a) Geometry of RC member (b) Proposed beam-column element including nonlinear connections with six degrees of freedom (c) The transformation points that subdivided RC element into some parts with constant flexural stiffness

and then with assuming the nonlinear behavior of the connections. Furthermore, to evaluate the proposed plasticity formulation, different number of element integration sections in Opensees software are applied. Comparing the consequences confirms the accuracy of the presented practical model.

2. Proposed beam-column element comprising joint flexibility

In the present study, a new RC beam-column element in which, distributed plasticity and nonlinear moment-rotation relation of joints are taken into account is developed. In order to simulate the joint flexibility, one zero-length rotational spring is attached at each end of the beam-column element and form the proposed beam-column element (Fig. 1).

In Fig. 1, M_A, V_A and N_A are the moment, shear and axial forces of end A, respectively and θ_A, v_A and u_A are its rotation and deformations of this end. The parameters of end B are similar to end A. k_{SA} and k_{SB} are the stiffness of rotational springs that are acquired according to the moment-rotation relationship that will be explained in this section. α_i is the i^{th} transformation point (the restricting locations along the structural elements according to flexibility change). EI_i and EI_m are current flexural stiffness of i^{th} and the last part, respectively. To develop the plasticity formulations, the methodology that was introduced by Izadpanah and Habibi (2018) is applied. It should be noted that the number of the divided parts in Fig. 1(c) depends on the degree of inelasticity along the RC element in each step of the analysis. The stiffness quantities that can be assigned to each part depend on the considered moment-curvature curve. The flexibility coefficients are derived from the principle of virtual work using the unit load method

$$f_{BB}=\frac{L'}{6}\left(\sum_{i=1}^{m-1}\left(\left(\frac{1}{EI_i}-\frac{1}{EI_{i+1}}\right)\times\left(2\propto_i^3\right)\right)+\frac{2}{EI_m}\propto_m^3\right)+\frac{1}{L'GA_z}+\frac{1}{k_{SB}} \tag{1}$$

$$f_{AA}=\frac{L'}{6}\left(\sum_{i=1}^{m-1}\left(\left(\frac{1}{EI_i}-\frac{1}{EI_{i+1}}\right)\times\left(6\propto_i^1-6\propto_i^2+2\propto_i^3\right)\right)+\frac{2}{EI_m}\times\left(6\propto_m^1-6\propto_m^2+2\propto_m^3\right)\right)+\frac{1}{L'GA_z}+\frac{1}{k_{SA}} \tag{2}$$

$$-f_{AB}=-f_{BA}=\frac{L'}{6}\left(\sum_{i=1}^{m-1}\left(\left(\frac{1}{EI_i}-\frac{1}{EI_{i+1}}\right)\times\left(3\propto_i^2-2\propto_i^3\right)\right)+\frac{1}{EI_m}\times\left(3\propto_m^2-2\propto_m^3\right)\right)-\frac{1}{L'GA_z} \tag{3}$$

GA_z is the shear stiffness of the element. This parameter is taken to be constant along the member. The inverse of the flexibility matrix is the stiffness matrix that it's components, including moment and shear deformations are calculated by Eqs. (4)-(10).

$$K_{AA}=\frac{3\prod_{i=1}^{m}EI_i}{L'D_{et}}\left(L'^2GA_zf'_{BB}+3\prod_{i=1}^{m}EI_i+\frac{\left(3\prod_{i=1}^{m}EI_i\right)GA_zL'}{k_{SB}}\right) \tag{4}$$

$$K_{BB}=\frac{3\prod_{i=1}^{m}EI_i}{L'D_{et}}\left(L'^2GA_zf'_{AA}+3\prod_{i=1}^{m}EI_i+\frac{\left(3\prod_{i=1}^{m}EI_i\right)GA_zL'}{k_{SA}}\right) \tag{5}$$

$$-K_{AB}=-K_{BA}=\frac{3\prod_{i=1}^{m}EI_i}{L'D_{et}}\left(L'^2GA_zf'_{AB}-3\prod_{i=1}^{m}EI_i\right) \tag{6}$$

$$D_{et}=L'^2GA_z\left(f'_{AA}f'_{BB}-{f'_{AB}}^2\right)+\frac{3\prod_{i=1}^{m}EI_i}{k_{SA}k_{SB}}\left(k_{SA}k_{SB}f'_{AA}+k_{SA}k_{SB}f'_{BB}+2k_{SA}k_{SB}f'_{AB}+L'GA_zf'_{AA}k_{SA}+L'GA_zf'_{BB}k_{SB}\right)+\frac{\left(3\prod_{i=1}^{m}EI_i\right)^2}{L'k_{SA}k_{SB}}\left(k_{SA}+k_{SB}\right)+\frac{1}{k_{SA}k_{SB}} \tag{7}$$

Where

$$f'_{BB}=\left(\sum_{j=1}^{m-1}\left(\prod_{\substack{i=1\\i\neq j}}^{m}EI_i-\prod_{\substack{i=1\\i\neq j+1}}^{m}EI_i\right)\propto_j^3\right)+\prod_{i=1}^{m-1}EI_i\propto_m^3 \tag{8}$$

$$f'_{AA}=\left(\sum_{j=1}^{m-1}\left(\prod_{\substack{i=1\\i\neq j}}^{m}EI_i-\prod_{\substack{i=1\\i\neq j+1}}^{m}EI_i\right)\left(3\propto_j^1-3\propto_j^2+\propto_j^3\right)\right)+\prod_{i=1}^{m-1}EI_i\left(3\propto_m^1-3\propto_m^2+1\propto_m^3\right) \tag{9}$$

$$f'_{AB}=\left(\sum_{j=1}^{m-1}\left(\prod_{\substack{i=1\\i\neq j}}^{m}EI_i-\prod_{\substack{i=1\\i\neq j+1}}^{m}EI_i\right)\left(\frac{3}{2}\propto_j^2-\propto_j^3\right)\right)+\prod_{i=1}^{m-1}EI_i\left(\frac{3}{2}\propto_m^2-\propto_m^3\right) \tag{10}$$

It is worth pointing out, these relations prepare the possibility of calculating the stiffness matrix of each beam-column element comprising the joint flexibility and the different flexibility properties along it. In this study, to achieve the transformation points, the moment distribution under the combination of the gravity and lateral loads is

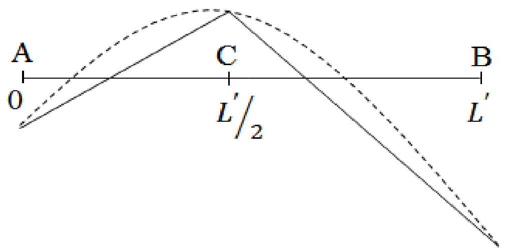

Fig. 2 Moment distribution of member and bilinear moment distribution

considered to be bilinear as depicted in Fig. 2. The moment distribution in previous models such as the linear, uniform and power plasticity models is assumed linear between two ends of a member that this assumption can bring about high approximation, as demonstrated by Izadpanah and Habibi (2015). In this research, to tackle this problem, the actual moment distribution (dashed line in Fig. 2) is approximated using bilinear that is more appropriate for the actual moment distribution of beams under a combination of gravity and lateral loads rather than the previous models.

To acquire the transformation points and flexibility of each part, three states of loading, unloading or reloading and transition to vertex are considered in hysteric model as detailed by Izadpanah and Habibi (2018).

To simulate the nonlinear behavior of connections, a simple analytical moment-rotation model proposed by Alva and El Debs (2013) is used to simulate the nonlinear response of the beam-column connections in the present study. According to Alva and El Debs (2013), the rotations between a RC beam and column are produced by the two mechanisms, as follows:

• Mechanism A: Relative rotations produced by the slippage of the beam reinforcement inside the joint.

• Mechanism B: Relative rotations produced by the cumulative effect of local slips caused by cracks opening in the beam next to the column along the length L_p (approximately the effective depth of the beam).

These researchers considered the moment-rotation curve of connection as shown in Fig. 3.

The proposed beam-column element has some advantages:

• The computational effort could be decreased using the proposed model, since it is capable of capturing the material nonlinearity along the entire length of a structural member and joint flexibility, even when employing a single element per member.

• The moment distribution is approximated using bilinear. This assumption for the exact moment distribution of beams under a combination of gravity and lateral loads is more appropriate than other assumptions considered in the previous models.

• A proposed general formulation prepares the possibility of computing the stiffness matrix for each flexibility distribution along the member. the proposed formulation is not dependent on assumed flexibility distribution. On the other hand, the stiffness matrix of each member with each assumption of flexibility along it can be calculated using the proposed formulations.

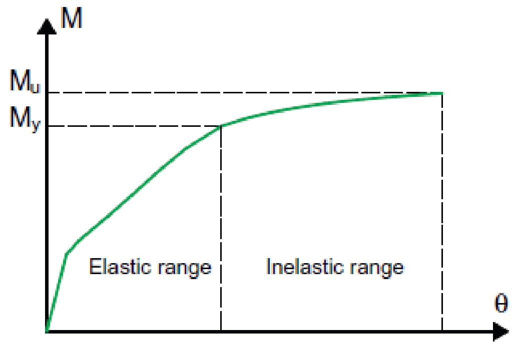

Fig. 3 Considered moment-rotation curve of connection (Alva and El Debs 2013)

• There is no requirement for calibration the entry parameters to simulate the joint deformability (Alva and El Debs 2013). Since the entry parameters of this model are the usual data for design of reinforced concrete elements, the aforementioned model can be easily implemented in the nonlinear analysis of framed structures with semi-rigid connections (Alva and El Debs 2013).

3. Analysis process

The nonlinear analysis is necessary to explain the actual behavior of the building frames. In this study, nonlinear static (pushover) and dynamic analyses of three reinforced concrete moment resistant frames are performed. The pushover analysis presents the comprehensive description of the entire behavior of frames from fully elastic to collapse. In pushover analysis, a predefined pattern of lateral loads is applied incrementally on the height of structure until a target displacement is reached or a plastic collapse mechanism takes place. The nonlinear dynamic analysis is carried out to evaluate the seismic behavior of the frames under earthquake ground motions. To perform nonlinear dynamic analysis, Newmark's method is utilized in the present research. The Newton-Raphson method is applied to the nonlinear analysis of structures. In this study, the nonlinear analysis of RC frames accounting for joint flexibility can be carried out in following steps:

• The tri-linear moment-curvature relation presented by Park *et al.* (1984) is adopted to determine the nonlinear behavior of RC sections. In the aforementioned moment-curvature relation, three states are presented, including the uncracked, cracked and yielded section properties that are distinguished using the cracking, yielding and ultimating moments and curvatures. The characteristic values of moment-curvature are calculated as follows:

a) Cracking moment and curvature

$$M_{cr} = \frac{f_r I}{(h-y)} + \frac{Nd}{6} \tag{11}$$

$$\varphi_{cr} = \frac{f_r}{E_c(h-y)} \tag{12}$$

b) Yielding moment and curvature

$$M_y = 0.5 f_c b_t d^2 (h-c)^2 [(1+\beta-\eta)n_0 + (2-\eta)\rho + (\eta - 2\beta)\alpha\rho'] \quad (13)$$

$$\varphi_{cr} = \frac{c\varepsilon_y}{d(1-k)} \quad (14)$$

c) Ultimate moment and curvature

$$M_u = (1.24 - 0.15p - 0.5n_0)M_y \quad (15)$$

$$\frac{\varphi_u}{\varphi_y} = \frac{\beta_1 \varepsilon_u E_s}{f_y} \frac{(1-k)}{\left(R^2 + S\frac{c}{d}\right) - \frac{R}{(h-c)}} \quad (16)$$

where $R = \frac{(\rho' \varepsilon_u E_s - \rho f_y)(h-c)}{(1.7 f_c)}$; $S = \frac{\rho' \varepsilon_u E_s \beta_1 c(h-c)}{(0.85 f_c)}$; f_r is the modulus of rupture of concrete; f_c is the cylinder strength of concrete; f_y is the yield strength of steel; E_c is the modulus of elasticity of concrete; E_s is the modulus of elasticity of steel; ω_u is the ultimate strain of concrete; ε_y is the yield strain of steel; β_1 is a coefficient that depends on the strength of concrete; h is the overall height of section; c is the cover to steel centroid; b_t is the top width of section; y is the distance from the neutral axis of the section to the extreme fiber in tension; I is the moment of inertia of the section. More details were presented in Ref. (Izadpanah 2017)

- The nonlinear moment-rotation curve of connections is derived based on the proposed relations by Alva and El Debs (2013).
- Shear and axial components, rigid zone effect and geometric stiffness matrix are added to the tangent stiffness matrix of each element using steps *a* to *e* (Habibi and Moharrami 2010).

a) Rigid zone effect is considered as follows

$$K'^{el}_{be} = \tilde{L} K^{el}_{be} L^{\sim -1}$$
$$K^{el}_{be} = \begin{bmatrix} K_{AA} & K_{AB} \\ K_{BA} & K_{BB} \end{bmatrix}; \quad (17)$$
$$[\tilde{L}] = \frac{1}{1-\lambda_a-\lambda_b} \begin{bmatrix} 1-\lambda_b & \lambda_b \\ \lambda_b & 1-\lambda_a \end{bmatrix}$$

where K^{el}_{be} is the stiffness matrix relating moments and rotations at the ends of the element that the components of it are achieved from Eqs. (4)-(10). λ_a and λ_b are the portions of rigid zone at the element ends.

b) The stiffness matrix considering force equilibrium of all the forces perpendicular to the axis of the element (K^{el}_b) is obtained as follows.

$$K^{el}_b = R_E{}^T K'^{el}_{be} R_E$$
$$R_E = \begin{bmatrix} -1/L & 1 & 1/L & 0 \\ -1/L & 0 & 1/L & 1 \end{bmatrix} \quad (18)$$

Where L is length of element.

c) The axial stiffness matrix of element (K^{el}_a) is obtained using Eq.(19) .

$$K^{el}_a = \frac{EA}{L}\begin{bmatrix} 1 & -1 \\ -1 & 1 \end{bmatrix} \quad (19)$$

Where $\frac{EA}{L}$ is the axial stiffness matrix of element.

a) The stiffness matrix of element comprising the axial and bending stiffness matrix ($K^{el}_t(6\times 6)$) is achieved as follows.

$$K^{el}_t = K^{el}_a + K^{el}_b \quad (20)$$

b) The geometrical stiffness matrix of element (the effect of second order terms in strain-displacement relation) is added to the element stiffness matrix and the final stiffness matrix of element is acquired.

$$K^{el}_f = K^{el}_t + K^{el}_g$$

Where

$$K^{el}_g = N/L \begin{bmatrix} 0 & & & & & \\ 0 & 6/5 & & \textit{symmetric} & & \\ 0 & L/10 & 2L^2/15 & & & \\ 0 & 0 & 0 & 0 & & \\ 0 & -6/5 & -L/10 & 0 & 6/5 & \\ 0 & L/10 & -L^2/30 & 0 & -L/10 & 2L^2/15 \end{bmatrix} \quad (21)$$

Where N is the axial force.

4. Numerical examples

To evaluate the efficiency and the applicability of the developed model, four numerical examples are considered. Pushover and Nonlinear Dynamic Analyses (NDA) are carried out on these examples. The first example is simply-supported test beam loaded at mid-span (Burns and Siess 1966). The second example is a ten-story, two-bay planner reinforced concrete moment resistant frame chosen from Habibi and Moharrami (2010). The third one is a three-story, three-bay planar reinforced concrete frame and the last one is a seven-story, three-bay planner reinforced concrete moment resistant frame selected from Habibi and Izadpanah (2012). The first example is under monotonic loading at mid-span. Pushover analysis is carried out on the second example. To analyze this example, the Proposed Distributed Flexibility Model (PDFM), the Linear Flexibility Model (LFM) and the Uniform Flexibility Model (UFM) are utilized. The beam-column connections are taken fully rigid in this example. To perform NDA, the two last aforementioned frames are once subjected to Northridge (the station 90019, component of 180) and after that a white noise acceleration record as depicted in Fig. 4. Two last frames are firstly analyzed using PDFM with assuming fully rigid beam-column connections. Afterwards, the joint flexibility is considered as illustrated in the section 2. To evaluate the validity of the presented methodology, the analyses are implemented again, using OpenSees software framework system (fiber-based analysis) (Mazzoni 2007). In OpenSees, to model structural elements, the nonlinearBeamColumn element with different number of integration points (The integration along the element is based on Gauss-Lobatto quadrature rule (Mazzoni 2007)) is taken.

4.1 Example 1

The first example is simply-supported test beam loaded at mid-span. The load-deflection responses for this beam under monotonic loading come from Burns and Siess

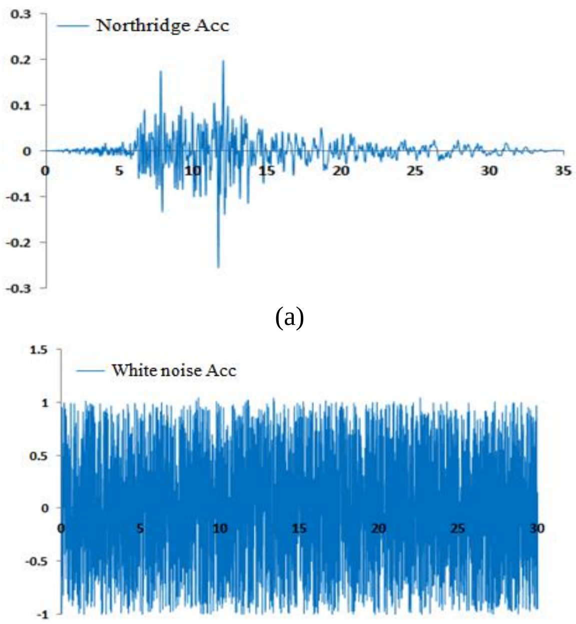

(a)

(b)

Fig. 4 Ground motions (a) Northridge (b) white noise

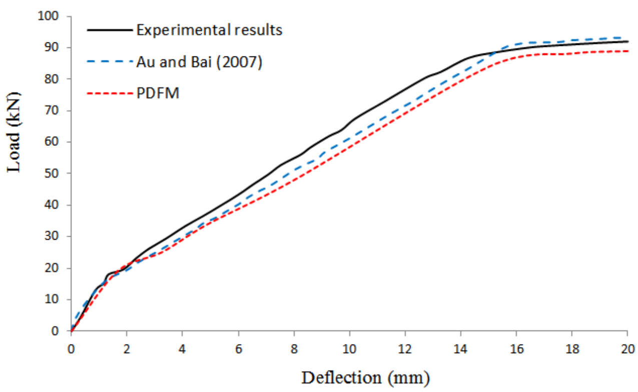

Fig. 5 Load-deflection curves

(1966) and finite element analysis was carried out by Au and Bai (2007). The total length and effective span of this beam are 3962 mm and 3658 mm, respectively. The width, height and effective height of beam are 203 mm, 305 mm and 245 mm, respectively. The concrete is assumed to have a cylinder strength of 34 MPa, a modulus of rupture of 3 MPa and a modulus of elasticity of 24500 MPa. The steel has a yield strength of 327 MPa and a modulus of elasticity of 200000 MPa. More details about the beam are achievable in Au and Bai (2007).

In this research, the PDFM formulations are applied to forecast the nonlinear behavior of this beam. The moment-curvature parameters for this beam are acquired using the relations that presented in section 3. To achieve the stiffness matrix, the Eqs. (4)-(10) are used. Fig. 5 compares the load-deflection responses of the aforementioned.

The high uncracked, cracked and yielded stiffness are observable for all load-deflection curves. Good agreement is observed between the PDFM results and the other results. It seems, the PDFM underestimate the inelastic response rather that experimental testing.

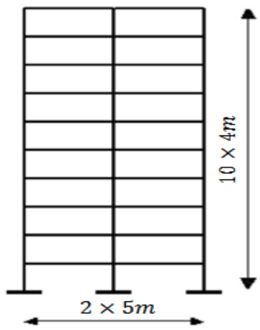

Fig. 6 Ten-story RC frame (Habibi and Moharrami 2010)

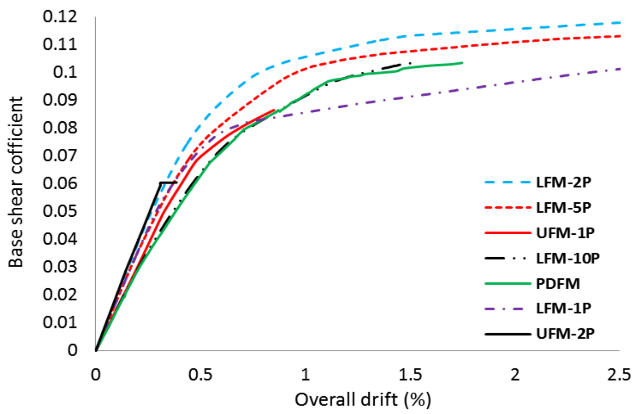

Fig. 7 Comparing the outcomes of PDFM with LFM-1P, LFM-5P, LFM-10P, UFM-1P and UFM-2P

4.2 Example 2

The second example is a ten-story, two-bay planner reinforced concrete moment resistant frame shown in Fig. 6 (Habibi and Moharrami 2010). The concrete is assumed to have a cylinder strength of 30 MPa, a modulus of rupture of 3.45 MPa, a modulus of elasticity of 27,400 MPa, a strain of 0.002 at maximum strength and an ultimate strain of 0.004. In this example, the difference in properties between confined core and cover is ignored. The steel has a yield strength of 300MPa and a modulus of elasticity of 200,000 MPa. More details are available in Ref. Habibi and Moharrami (2010).

The distributed gravity load imposed on the beams is considered 35 kN/m. LFM and UFM are used to analyze this example, several times. In the first one, each beam is considered as one element (named afterward LFM-1P, UFM-1P). In the other ones, members are subdivided into two, five and ten parts (hereafter referred to as LFM-2P, LFM-5P, LFM-10P and UFM-2P). After the aforementioned analyses, the suggested formulation is utilized to perform pushover analysis. The results of these analyses are described in Fig. 7.

As presented in Fig. 7, UFM-1P and UFM-2P experience failure state before overall drift 1 and 0.5 percent, respectively. Not separating cracked and yielded length in uniform flexibility model is the cause of these failures because as soon as the end moment of member exceeds the yielding moment, the stiffness of the cracked length of the aforementioned end will be equal to the

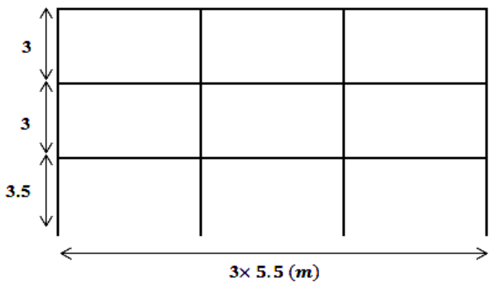

Fig. 8 Three-story RC frame

Table 1 The cross section properties of three-story RC frame

Element type	Dimension (mm)		Reinforcement	
Beam	Width	Height	Bottom	Top
All beams	400	400	4∅20	6∅20
Column	Dimension (mm)		Reinforcement on each face	
	Width	Height		
Edge columns	400	400	4∅28	
Middle columns	450	450	4∅30	

yielding stiffness. The gap between LFM-1P and PDFM increases for inelastic deformations. Comparing the results of linear flexibility model and proposed distributed plasticity model shows that better compliance will be achieved when more subdivided elements for each member is used (The LFM-10P has the best compliance with PDFM.). On the other hand, using more elements for linear flexibility model, the approximation of this model will decrease; therefore, converging the results of proposed model to LFM-10P present the accuracy of it.

4.3 Example 3

The third example is a three-story, three-bay planner reinforced concrete moment resistant frame (Fig. 8). The concrete is assumed to have a cylinder strength of 28 MPa and 24 MPa, a strain of 0.0022 and 0.002 at maximum strength and an ultimate strain of 0.007 and 0.0035 in core and cover, respectively. The steel has a yield strength of 400 MPa and a modulus of elasticity of 200,000 MPa. The considered materials are Concrete02 and Steel02. Each cross section is divided into core and cover that are subdivided into small fibers. A uniformly distributed gravity load of 14 kN/m is applied on the beam. It is assumed that columns and beams have rectangular cross sections detailed in Table 1. Pushover and nonlinear dynamic analyses are carried out on this frame assuming rigid connection and using PDFM. After that, the analyses are accomplished once more using OpenSees (nonlinearBeamColumn element) that the number of element's integration sections is considered three, four and ten (denoted afterward 3-NP, 4-NP and 10-NP). The Gauss-Lobatto quadrature rule is used for the aforementioned integration sections. The moment-curvature properties in PDFM are similar to what are achieved using OpenSees based on fiber-section method. On the other hand, the obtained moment-curavature properties of Opensees are considered as input parameters for PDFM (to

Table 2 The moment-curvature components of three-story RC frame (kN.m , 1/m)

Element type	M_{cr}		φ_{cr}		M_y		φ_y		M_u		φ_u	
Beam	+	-	+	-	+	-	+	-	+	-	+	-
All beams	35	70	0.002	0.003	145	212	0.01	0.011	156	227	0.06	0.1
Column												
Edge columns	93		0.003		288		0.011		316		0.06	
Middle columns	147		0.003		392		0.01		442		0.06	

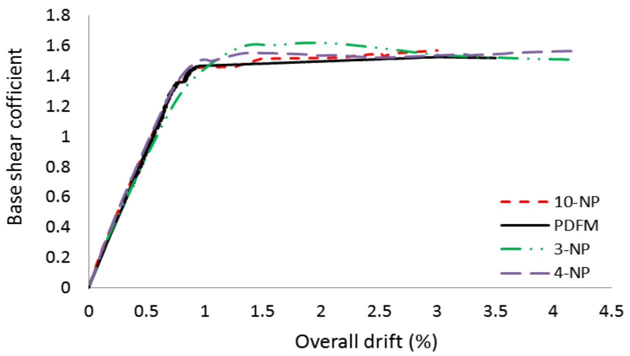

Fig. 9 Capacity curves of the three-story, three-bay frame

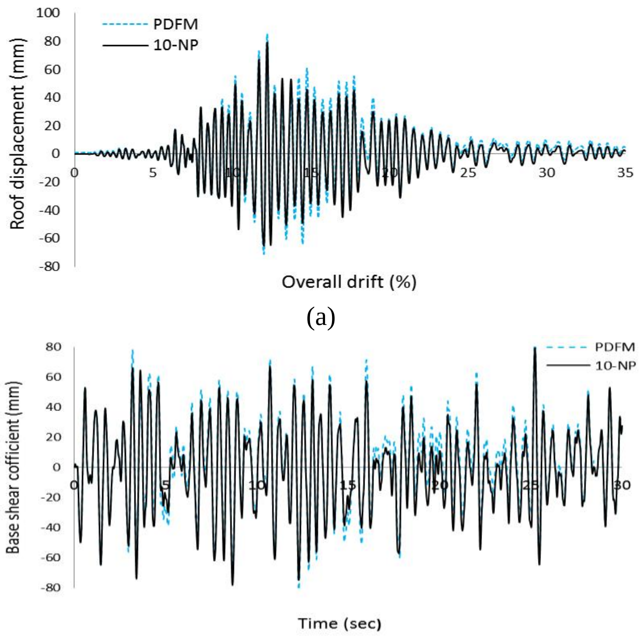

(a)

(b)

Fig. 10 Roof displacement for considered ground motions (a) Northridge (b)White noise

prepare the same condition for comparing the results). These properties are summarized in Table 2. For nonlinear dynamic analysis, Northridge with PGA 0.93 g and White noise with 1.12 g are considered. The outcomes of the above mentioned analyses are presented in Figs. (9)-(10).

As demonstrated in Fig. 9, by increasing the number of element's integration sections, the gap between the results of OpenSees with those of PDFM will decrease (10-NP has

Table 3 The moment-rotation properties of beam to column connections of three-story RC frame (kN.m)

M_{cr}		θ_{cr}		M_y		θ_y		M_u		θ_u	
+	-	+	-	+	-	+	-	+	-	+	-
35	70	5.65e-4	8.55e-4	145	212	0.0039	0.0042	156	227	0.0281	0.0256

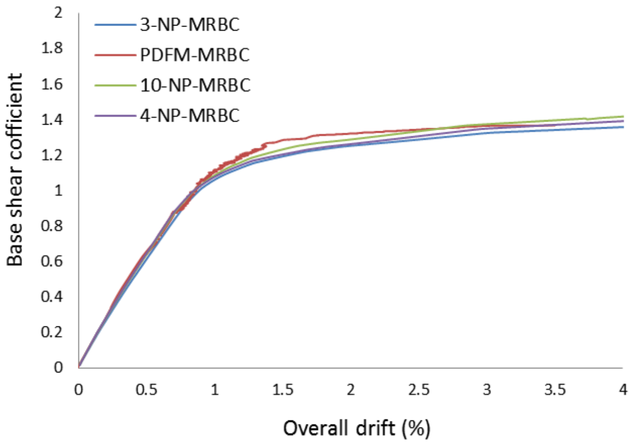

Fig. 11 Capacity curves of the three-story, three-bay frame with nonlinear connections

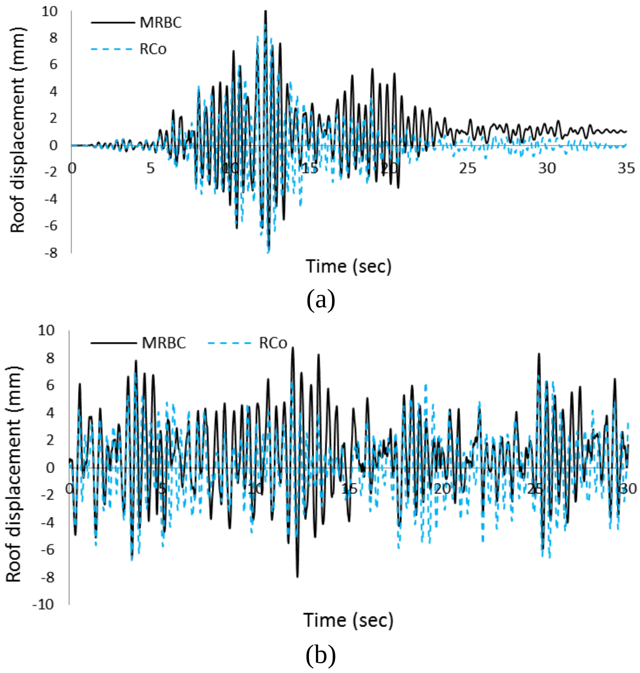

Fig. 12 Roof displacement of three-story frame MRBC and RCo under considered ground motions (a) Northridge (b) White noise

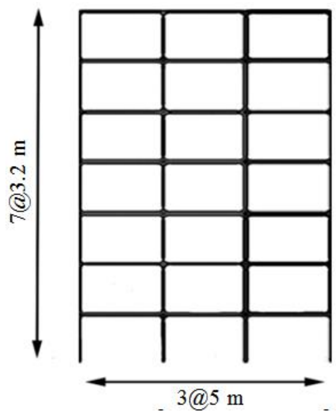

Fig. 13 Geometry of seven-story RC frame

the best compliance with PDFM). Comparing consequences shows by increasing the number of element's integration sections, the results of OpenSees are converged to PDFM. Contrasting the results of the nonlinear dynamic analyses confirms the accuracy of PDFM (Fig. 10). For Northridge record, the peak of roof displacement for PDFM is 85 mm and for 10-NP is 79 mm. It seems, both models experience small permanent deformation after 25 seconds of the analysis. For white noise ground motion, the maximum roof displacement is 89 mm and 80 mm for PDFM and 10-NP, respectively. After the aforementioned analyses, the joint nonlinearity properties of this frame are calculated using the proposed relations by Alva and El Debs (2013). It is worth emphasizing that the obtained moment-rotation properties of beam-column connections are tabulated in Table 3.

The analyses are performed once using the developed beam-column element in section 2 and again with OpenSees. In OpenSees, zero-length element is used to model the nonlinear connections. The results of pushover analysis on the aforementioned frame by assuming moment-rotation relationship of beam-column connections (hereafter referred to as MRBC) are presented in Fig. 11. To compare the seismic response of this example with rigid connections (hereafter referred to as RCo) and nonlinear behavior of beam-column connections (MRBC), the nonlinear dynamic analysis is carried out under Northridge with PGA 0.12 g and White noise with 0.12 g ground motions. Outcomes are depicted in Fig. 12.

As it is evident in Fig. 11, the outcome of the proposed beam-column element, including joint flexibility is compatible with the nonlinearBeamColumn element with ten of integration points (10-NP). Contrasting roof displacement in Fig. 12 shows that although the peak of top displacements for frame with assuming RCo and MRBC are close, frame with nonlinear connections endures permanent deformations.

4.4 Example 4

Seven-story, three-bay planner reinforced concrete moment resistant frame as the fourth example is evaluated in this study (Fig. 13) (Habibi and Izadpanah 2012). Rectangular cross sections are considered for all beams and columns as detailed in Table 4. Concrete cylinder strength of 38 MPa for core and 30 MPa for cover are taken into account. A strain of 0.0022 and 0.002 at maximum strength of concrete and an ultimate strain of 0.006 and 0.003, are assumed in core and cover; respectively. The steel has a yield strength of 300 MPa and a modulus of elasticity of 200,000 MPa. More details are achievable in Ref. Habibi and Izadpanah (2012). Similar to the third example, Concrete02 and Steel02 are assigned to the materials and each cross section is divided into core and cover that are

Table 4 The cross section properties of seven-story RC frame

Element type	Dimension (mm)		Reinforcement	
Beam	Width	Height	Bottom	Top
1st to 5th story	300	450	3∅20	7∅20
6th and 7th story	350	400	3∅20	4∅20
Column	Dimension (mm)		Reinforcement on each face	
	Width	Height		
1st story	500	500	7∅20	
2nd and 3rd story	500	500	6∅20	
4th and 5th story	450	450	5∅20	
6th and 7th story	350	350	5∅20	

Table 5 The moment-rotation properties of beam-to-column connections of seven-story RC frame (kN.m)

Story	M_{cr}		θ_{cr}		M_y		θ_y		M_u		θ_u	
	+	-	+	-	+	-	+	-	+	-	+	-
1st to 5th	10.4	23.7	1.39e-4	1.51e-4	100	221	0.002	0.0022	119	250	0.0195	0.0153
6th and 7th	9.4	12	1.57e-4	1.59e-4	88.5	116	0.0023	0.0021	103	169	0.0196	0.0663

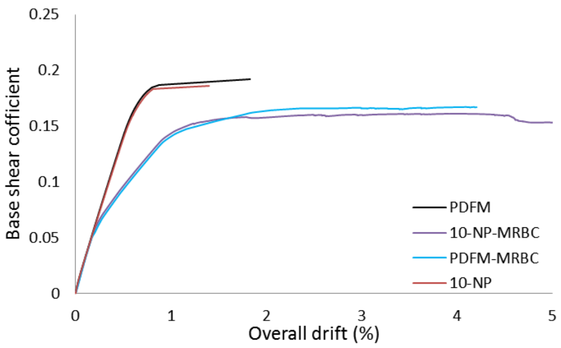

(a)

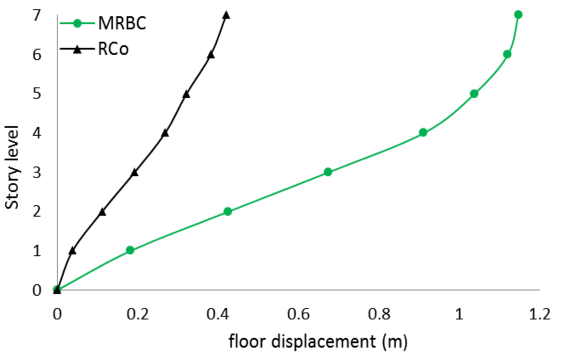

(b)

Fig. 14 Displacement outcomes of the seven-story, three-bay frame with RCo and MRBC (a) Capacity curves (b) final floor displacement

subdivided into small fibers. The moment-curvature properties in PDFM are similar to what are achieved using OpenSees based on fiber-section method. All beams are subjected to a uniformly distributed gravity load of 30

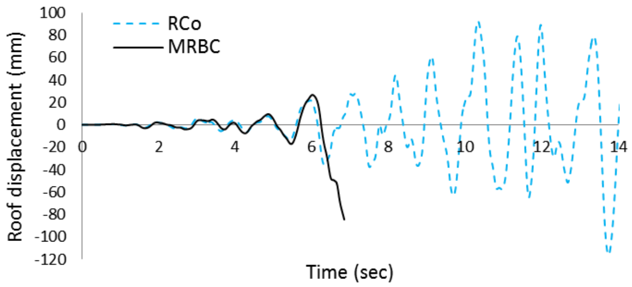

(a)

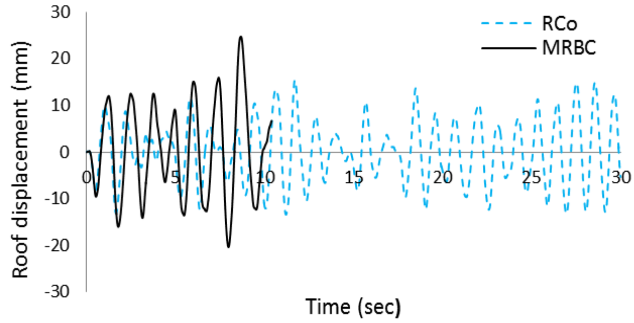

(b)

Fig. 15 Roof displacement of seven-story frame with rigid and RCo under considered ground motions (a) Northridge (b) White noise

kN/m. Pushover analysis is done on this frame assuming RCo and MRBC using PDFM as well as nonlinear Beam Column element with ten of element's integration sections (OpenSees). The joint flexibility properties are presented in Table 5. The capacity curves acquired from pushover analysis are presented in Fig. 14(a). The final floor displacements of both frames (RCo and MRBC) are described in Fig. 14(b).

As exhibited, the results of PDFM and 10-NP as well as PDFM-MRBC and 10-NP- MRBC are in good agreement. The peak of base shear coefficient for the MRBC is 80 percent of RCo approximately. The ductility for MRBC is more than RCo. The maximum percentage of overall drift for MRBC is around 5 whereas for RCo is almost 2. For both frames, difference between floor displacements (drift) is decreased for top stories (Fig. 14(b)). In Fig. 15, the nonlinear dynamic responses for this example with taking rigid connections and joint flexibility are compared. For these analyses, Northridge with PGA 0.91 g and White noise with 0.06 g are taken into account.

Contrasting the outcomes in Fig. 15(a) demonstrates that both frames experience failure. As it is expected, frame with MRBC failed earlier than RCo. For White noise ground motion (Fig. 15(b)), the peak of top story displacement of the frame with rigid connections is almost 15 mm, whereas the frame with joint flexibility experiences failure.

5. Conclusions

A new RC beam-column element in which distributed plasticity and nonlinear behavior of beam-column connections are taken into account is proposed in this study.

The nonlinear behavior of the connections comprising relative rotations produced by the slippage of the beam reinforcement inside the joint and also cumulative effect of local slips caused by cracks opening are taken into account. Moreover, in the presented spread plasticity model, the gravity and the lateral load effects are considered, simultaneously. To confirm the accuracy of the developed plasticity model, four numerical examples are evaluated. The following conclusions can be outlined from this research:

• While the proposed RC beam-column element use one element for each member, it can simulate the influences of the relative slip of flexural reinforcement in the joint and also the flexural cracking of the beam end on the relative rotation of beam-column connections. Furthermore, the distribution of material nonlinearity along the member in the presented beam-column element is considered well.

• In the uniform plasticity model, not separating the cracked and yielded lengths cause wrong responses.

• The nonlinear behavior of the beam-column connections plays an outstanding role in the structural response in pushover and nonlinear dynamic analysis. The lateral load bearing capacity of RC frames is reduced when the nonlinear behavior of connections is simulated.

• In seismic motions, when the nonlinear behavior of connections is simulated, RC frames experience smaller displacement rather than those with rigid connections.

References

Alameddine, F. and Ehsani, M.R. (1991), "High strength RC connections subjected to inelastic cyclic loading", *J. Struct. Eng*., **117**(3), 829-50.

Altoontash, A. and Deierlein, G.D. (2003), "A versatile model for beam-column joints", *Proceedings of the ASCE Structures Congress*, Seattle, WA.

Alva, G.M.S. and de Cresce, El, A.L.H. (2013), "Moment-rotation relationship of RC beam-column connections: Experimental tests and analytical model", *Eng. Struct.*, **56**, 1427-1438.

Amorim, D.L.D.F., Proença, S.P. and Flórez-López, J. (2013), "A model of fracture in reinforced concrete arches based on lumped damage mechanics", *Int. J. Solid. Struct.*, **50**(24), 4070-4079.

Au, F.T.K. and Bai, Z.Z. (2007), "Two-dimensional nonlinear finite element analysis of monotonically and non-reversed cyclically loaded RC beams", *Eng. Struct*., **29**(11), 2921-2934.

Babazadeh, A., Burgueño, R. and Silva, P.F. (2016), "Evaluation of the critical plastic region length in slender reinforced concrete bridge columns", *Eng. Struct*., **125**, 280-293.

Berry, M.P., Lehman, D.E. and Lowes, L.N. (2008), "Lumped-plasticity models for performance simulation of bridge columns", *ACI Struct. J*., **105**(3), 270-279.

Birely, A.C., Lowes, L.N. and Lehman, D.E. (2012), "A model for the practical nonlinear analysis of reinforced-concrete frames including joint flexibility", *Eng. Struct*., **34**, 455-465.

Burns, N.H. and Siess, C.P. (1966), "Plastic hinging in reinforced concrete", *J. Struct. Div. Pr.*, ASCE, **92**(5), 45-64.

Filippou, F.C., D'Ambrisi, A. and Issa, A. (1992), "Nonlinear static and dynamic analysis of reinforced concrete subassemblages", Report No. UCB/EERC-92/08, Earthquake Engineering Research Center.

Filippou, F.C., Popov, E.P. and Bertero, V.V. (1983), "Effects of bond deterioration on hysteretic behavior of reinforced concrete joints", Report No. UCB/EERC-83/19, Earthquake Engineering Research Center.

Ghobarah, A. and Biddah, A. (1999), "Dynamic analysis of reinforced concrete frames including joint shear deformation", *Eng. Struct*., **21**(11), 971-87.

Gu, Q., Barbato, M., Conte, J.P., Gill, P.E. and McKenna, F. (2011), "OpenSees-SNOPT framework for finite-element-based optimization of structural and geotechnical systems", *J. Struct. Eng*., **138**(6), 822-834.

Habibi, A. and Moharrami, H. (2010), "Nonlinear sensitivity analysis of reinforced concrete frames", *Finite Elem. Anal. Des*., **46**(7), 571-584.

Habibi, A.R. (2008), "Optimal seismic performance based design of 2D reinforced concrete frames", Ph.D. Thesis, Tarbiat Modarres Univ., Tehran, Iran.

Habibi, A.R. and Izadpanah, M. (2012), "New method for the design of reinforced concrete moment resisting frames with damage control", *Scientia Iranica*, **19**(2), 234-241.

He, R. and Zhong, H. (2012), "Large deflection elasto-plastic analysis of frames using the weak-form quadrature element method", *Finite Elem. Anal. Des.*, **50**, 125-133.

Inel, M. and Ozmen, H.B. (2006), "Effects of plastic hinge properties in nonlinear analysis of reinforced concrete buildings", *Eng. Struct*., **28**(11), 1494-1502.

Ismail, R. and Zamahidi, N.F. (2015), "An evaluation of high-rise concrete building performance under low intensity earthquake effects", *InCIEC 2014*, 79-86.

Izadpanah, M. and Habibi, A. (2015), "Evaluating the spread plasticity model of IDARC for inelastic analysis of reinforced concrete frames", *Struct. Eng. Mech*., **56**(2), 169-188.

Izadpanah, M. and Habibi, A.R. (2018), "New spread plasticity model for reinforced concrete structural elements accounting for both gravity and lateral load effects", *J. Struct. Eng*., **144**(5), 04018028.

Izadpanah. M. (2017), "A new plasticity model for beam-column element to take into account the influence of lateral and gravity loads", Ph.D. Thesis, Structural Engineering, University of Kurdistan.

Izzuddin, B.A., Karayannis, C.G. and Elnashai, A.S. (1994), "Advanced nonlinear formulation for reinforced concrete beam-columns", *J. Struct. Eng*., **120**(10), 2913-2934

Kim, S.P. and Kurama, Y.C. (2008), "An alternative pushover analysis procedure to estimate seismic displacement demands", *Eng. Struct*.. **30**(12), 3793-3807.

Kitayama, K., Otani, S. and Aoyama, H. (1987), "Earthquake resistant design criteria for reinforced concrete interior beam-column joints", *Proceedings of the Pacific Conference on Earthquake Engineering*, Wairakei, New Zealand.

Kunnath, S.K. and Reinhorn, A.M. (1989), "Inelastic three-dimensional response analysis of reinforced 676 concrete building structures (IDARC-3D)", National Center for Earthquake Engineering Research, State 677 University of New York at Buffalo.

Kwak, H.G. and Kim, S.P. (2010), "Simplified monotonic moment-curvature relation considering fixed-end rotation and axial force effect", *Eng. Struct*., **32**, 69-79.

Lee, C.L. and Filippou, F.C. (2009), "Efficient beam-column element with variable inelastic end zones", *J. Struct. Eng*., **135**(11), 1310-1319.

Lee, H.S. and Woo, S.W. (2002), "Seismic performance of a 3-story RC frame in a low-seismicity region", *Eng. Struct*., **24**(6), 719-734.

Lowes, L.N. and Altoontash, A. (2003), "Modeling reinforced-concrete beam-column joints subjected to cyclic load", *J. Struct. Eng*., **129**(12), 1686-97.

Mashaly, E., El-Heweity, M., Abou-Elfath, H. and Osman, M. (2011), "Finite element analysis of beam-to-column joints in steel frames under cyclic loading", *Alexandria Eng. J.*, **50**(1), 91-104.

Masi, A., Santarsiero, G., Lignola, G.P. and Verderame, G.M. (2013), "Study of the seismic behavior of external RC beam-column joints through experimental tests and numerical simulations", *Eng. Struct.*, **52**, 207-219.

Mazza, F. (2014), "A distributed plasticity model to simulate the biaxial behaviour in the nonlinear analysis of spatial framed structures", *Comput. Struct.*, **135**, 141-154.

Mazzoni, S., McKenna, F., Scott, M.H. and Fenves, G.L. (2006), *OpenSees Command Language Manual*.

Mergos, P.E and Kappos, A.J. (2012), "A gradual spread inelasticity model for R/C beamcolumns, accounting for flexure, shear and anchorage slip", *Eng. Struct.*, **44**, 94-106.

Mitra, N. and Lowes, L.N. (2007), "Evaluation, calibration, and verification of a reinforced concrete beam-column joint", *J. Struct. Eng.*, **133**(1), 105-120.

Monti, G., Filippou, F.C. and Spacone, E. (1997), "Finite element for anchored bars under cyclic load reversals", *J. Struct. Eng.*, **123**(5), 614-23.

Nguyen, P.C. and Kim, S.E. (2014), "Distributed plasticity approach for time-history analysis of steel frames including nonlinear connections", *J. Constr. Steel Res.*, **100**, 36-49.

Pan, W.H., Tao, M.X. and Nie, J.G. (2016), "Fiber beam-column element model considering reinforcement anchorage slip in the footing", *Bull. Earthq. Eng.*, **15**(3), 991-1018.

Park, R. and Ruitong, D. (1998), "A comparison of the behavior of reinforced concrete beam column joints designed for ductility and limited ductility", *Bull. NZ. Nat. Soc. Earthq. Eng.*, **21**(4), 255-278.

Paulay, T. and Scarpas, A. (1981), "The behaviour of exterior beam-column joints", *Bull. NZ. Nat. Soc. Earthq. Eng.*, **14**(3), 131-144

Paultre, P., Castele, D., Rattray, S. and Mitchell, D. (1989), "Seismic response of reinforced concrete frame subassemblages - a Canadian code perspective", *Can. J. Civil Eng.*, **16**, 627-649.

Rahai, A.R. and Nafari, S.F. (2013), "A comparison between lumped and distributed plasticity approaches in the pushover analysis results of a pc frame bridge", *Int. J. Civil Eng.*, **11**(4), 217-225.

Reinhorn, A.M., Roh, H., Sivaselvan, M., Kunnath, S.K., Valles, R.E., Madan, A., Li, C., Lobo, R. and Park, Y.J. (2009), "IDARC 2D Version 7.0: A Program for the Inelastic Damage Analysis of Structures", MCEER Technical Report- MCEER-09-0006, University at Buffalo-the State University of New York.

Roh, H., Reinhorn, A.M. and Lee, J.S. (2012), "Power spread plasticity model for inelastic analysis of reinforced concrete structures", *Eng. Struct.*, **39**, 148-161.

Russo, G., Zingone, G. and Romano, F. (1990), "Analytical solution for bond-slip of reinforced bars in R.C. joints", *J. Struct. Eng.*, **116**(2), 336-355.

Scott, M.H. and Fenves, G.L. (2006), "Plastic hinge integration methods for force-based beam-column elements", *J. Struct. Eng.*, **132**(2), 244-252.

Scott, M.H., Fenves, G.L., McKenna, F. and Filippou, F.C. (2008), "Software patterns for nonlinear beam-column models", *J. Struct. Eng.*, **134**(4), 562-571.

Sezen, H. and Moehle, J.P. (2003), "Bond-slip behavior of reinforced concrete members", *Fib-Symposium (CEB-FIP)-Concrete Structures in Seismic Regions*, Athens, Greece.

Sezen, H. and Setzler, E.J. (2008), "Reinforcement slip in reinforced concrete columns", *ACI Struct. J.*, **105**(3), 280-289.

Shafaei, J., Zareian, M.S., Hosseini, A. and Marefat, M.S. (2014), "Effects of joint flexibility on lateral response of reinforced concrete frames", *J. Struct. Eng.*, **81**, 412-431.

Sivaselvan, M.V. and Reinhorn, A.M. (2000), "Hysteretic models for deteriorating inelastic structures", *J. Eng. Mech.*, **126**(6), 633-640.

Sun, X.J., Cao, J.P. and Zheng, W.Z. (2011), "Seismic elastic-plastic analysis on Outer-Jacketing mega frame for story-adding by IDARC-2D", *Adv. Mater. Res.*, **255**, 209-214.

Tsonos, A.D.G. (2010), "Performance enhancement of R/C building columns and beam-column joints through shotcrete jacketing", *Eng. Struct.*, **32**(3), 726-740.

Tsonos, A.G. (2007), "Cyclic load behavior of reinforced concrete beam-column subassemblages of modern structures", *ACI Struct. J.*, **104**(4), 468-475.

Tsonos, A.G. (2008), "Effectiveness of CFRP-jackets and RC-jackets in post-earthquake and pre-earthquake retrofitting of beam-column subassemblages", *Eng. Struct.*, **30**(3), 777-793.

Walker, S.G. (2001), "Seismic performance of existing reinforced concrete beam-column joints", Doctoral Dissertation, University of Washington.

Zhao, J. and Sritharan, S. (2007), "Modeling of strain penetration effects in fiber-based analysis of reinforced concrete structures", *ACI Struct. J.*, **104**(2), 133-141.

Zhao, X.M., Wu, Y.F. and Leung, A. (2012), "Analyses of plastic hinge regions in reinforced concrete beams under monotonic loading", *Eng. Struct.*, **34**, 466-482.

AT